

phys. stat. sol. (a) 1, 409 (1970)

Subject classification: 14.3.1 and 14.4.1; 22

*School of Physical Sciences, New University of Ulster,
Coleraine, Northern Ireland*

Thermally Assisted Tunnelling in Dielectric Films

By

G. G. ROBERTS and J. I. POLANCO

A tunnelling mechanism is described which considers the situation where the major contribution to the tunnelling integral comes, not from the region of the Fermi level, but from an energy position located some way above this energy. At the same time this tunnelling mechanism dominates over the electron transfer which proceeds at levels above the barrier. The theoretical curves presented for thermally assisted tunnelling (TAT) show it to be a mechanism that must always be considered in investigations of thin film dielectrics. For appropriate parameters, TAT yields the same shape current-voltage characteristic as Schottky emission or the Poole-Frenkel effect, but may be distinguished by the weak temperature and field dependence of its pre-exponential factor.

Ein Tunnelmechanismus wird beschrieben, der den Fall berücksichtigt, daß der Hauptanteil zum Tunnelintegral nicht aus dem Bereich des Fermi-niveaus kommt, sondern von einem Energiebereich, der sich um einiges über dieser Energie befindet. Zur gleichen Zeit dominiert dieser Tunnelmechanismus über den Elektronentransport, der an Niveaus oberhalb des Potentialwalls erfolgt. Die abgebildeten theoretischen Kurven für TAT (thermisch unterstützte Tunnelung) beweisen, daß dieser Tunnelmechanismus immer bei Untersuchungen von nichtleitenden dünnen Schichten berücksichtigt werden muß. Für die zugehörigen Parameter liefert die TAT die gleiche Stromspannungscharakteristik wie die Schottky-emission oder der Poole-Frenkel-Effekt, kann aber durch die geringe Temperatur- und Feldabhängigkeit des vorexponentiellen Faktors unterschieden werden.

1. Introduction

An understanding of the conduction mechanism across a thin layer of dielectric is pertinent to the development and operation of thin film practical devices. Accordingly, in recent years, a well defined field of study has developed in connection with the electrical properties of an insulating layer sandwiched between two metals. A predominant feature of these investigations is the very high field strengths that are involved and, in many situations, the negligible dependence on sample bulk conductivity.

When the insulator is very thin, the conduction process is dominated by a potential barrier analogous to that which exists at a metal-vacuum interface. Tunnelling and Schottky thermionic emission are generally regarded as the two most important conduction mechanisms under these conditions. Several theorists have calculated the critical dependence of the shape of the potential barrier on the current-voltage characteristics and have included such effects as image forces [1], space charge [2 to 5], ionic defects [6], electric field penetration of the electrodes [7], trapping [8, 9] and thickness fluctuations [10] in their analyses. Some of these theories are reviewed in the monograph by Lamb [11]. Many of the modifications were suggested to help explain certain discrepancies that exist between experimental results and theory. There are, for

example, several reports in the literature of current-voltage curves exhibiting the functional form expected for Schottky behaviour (a linear $\log J$ versus $U^{1/2}$ plot) but whose pre-exponential factors differ from theoretically predicted values, being more characteristic of a tunnelling than a thermally activated process. O'Dwyer [12] has proposed a model based on Fowler-Nordheim tunnelling and thermal and field excitation of deep electrons into shallow traps and the conduction band to explain such discrepancies, while McColl and Mead [13] have suggested that polaron states in the insulator could be responsible for such effects. For ionic solids, Emtage [14] has considered the contribution of longitudinal optical phonons to the tunnelling process.

We present in this paper a tunnelling mechanism which serves as an alternative explanation for some of the anomalous experimental results observed. It describes the situation where the major contribution to the tunnelling integral comes not from the region of the Fermi level but from an energy position located some way above this energy. At the same time this tunnelling mechanism dominates over the thermal electron transfer which proceeds at levels above the barrier. The theoretical curves presented for thermally assisted tunnelling (TAT) show it to be a mechanism that must always be considered in investigations of thin film dielectrics. This effect should not be confused with the mechanism of tunnelling through potential barriers whose thickness varies due to lattice vibrations in the solid. The theory for this problem, which applies to low mobility materials, has been discussed by other authors [15, 16] and has also been termed thermally assisted tunnelling.

2. Summary of Existing Thin-Film Conduction Mechanisms

Fisher and Giaever's [17] experimental results on Al_2O_3 are usually quoted as an illustration of direct quantum mechanical tunnelling in very thin films. The current in this case is characterized by a weak temperature dependence and a barrier transmission coefficient $P(\Phi, s)$ which depends on both the height of the barrier, Φ , and its thickness, s . The direct tunnelling theories of Sommerfeld and Bethe [18] have been extended in recent years to include barriers of arbitrary shape. Stratton [19], in particular, has obtained a general expression, valid at low current densities, which McColl and Mead [13] have shown to be in quantitative agreement with the voltage and temperature dependence of tunnelling currents in thin films of mica. For low applied voltages ohmic behaviour is predicted while for high fields the following relationship is a good approximation,

$$J = \alpha U^2 e^{-\beta/U}, \quad (1)$$

where α and β are constants.

Emtage and Tantraporn [20] attributed the current transfer through thin insulating films of polymerized silicon oil to the emission of electrons from the cathode into the conduction band of the dielectric over the interfacial barrier, in a manner analogous to Schottky emission in a vacuum. This effect is characterized by a linear relation between the logarithm of the current and the square root of the applied voltage:

$$J = \gamma e^{\delta U^{1/2}}, \quad (2)$$

where $\delta = (e^3/\kappa s)^{1/2}/kT$ and $\gamma = A T^2 \exp(-\Phi/kT)$.

In this equation Φ represents the metal-insulator work function, A is Richardson's constant; κ and s are the dielectric constant and thickness respectively of the insulating film. Clearly thermionic emission is strongly dependent on both barrier height and temperature and may thus be distinguished from a direct tunnelling mechanism. Pollack [21] has shown that it is possible for both Schottky and tunnel emission to be simultaneously responsible for the passage of large currents in thin film dielectrics.

Measurements on thicker layers tend to show the influence of bulk phenomena and complicated effects such as multiple trapping. (A situation involving the ratio of free to trapped charge would certainly be temperature dependent and this could mask the possible temperature independence of the generation mechanism.) For example, there are several reports of space charge limited currents in thin film structures [22, 23] a mechanism which it is fairly easy to isolate from other causes of non-ohmic behaviour. The Poole-Frenkel effect, the electric field assisted thermal ionization of trapped charge carriers, has also been observed [9]. It transpires that the functional dependence of the current on applied field strength is identical for the Schottky and Poole-Frenkel mechanisms. However, the barrier lowering in the latter is twice that observed in the former and consequently the constant involved in the exponent may differ from the value δ . A recent three dimensional calculation by Hartke [24] and the predictions of theoretical models proposed by Simmons [8] and Yeargan and Taylor [9] based on the degree of compensation in the bulk of the dielectric, are possible explanations why experimental results yield slopes that fall between the estimated Poole-Frenkel dependence and that expected for Schottky emission.

Larger discrepancies exist between experimental results and theory than simply a factor of two. For example, in some situations where the current flow increases exponentially with the square root of the applied voltage, δ , has been found to be essentially temperature independent, [25, 26] thereby invalidating Schottky behaviour as the conduction mechanism involved. A mechanism based on Fowler-Nordheim tunnelling proposed by O'Dwyer [12] is insufficient to explain this anomaly, for, although his computer curves show regions in which $\log J \sim U^{1/2}$, his model is incomplete in that it does not include a temperature dependent current term. Lilly et al. [27] have recently explored the model in some detail and have found that its low current-low field limit severely restricts its range of applicability. Furthermore, from their extensive investigation they concluded that for realistic parameters in O'Dwyer's model, the shape of a pure Schottky curve cannot be obtained. McColl and Mead [13], Hirose and Wada [28], Hartman et al. [29] have all found that, in attempting to fit their experimental curves to a Schottky plot, differences exist between predicted dielectric constant values and those obtained from other measurements. Polaron states in the insulator have been invoked to explain anomalies in thermal activation energy determinations [13].

3. Thermally Assisted Tunnelling

The conduction processes through a dielectric film depend critically upon the shape of the potential barrier in the insulator. If a rectangular barrier model is used to approximate the barrier shape, the schematic energy diagram of Fig. 1, for a sandwich of two metallic electrodes separated by a film, results from the application of a bias voltage U . Geppert [2] has computed the effect of space

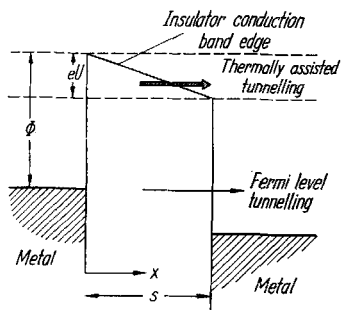


Fig. 1. Schematic representation of the energy bands of a metal-insulator-metal diode resulting from the application of a bias voltage U

charge due to free carriers in the barrier and has shown that it is negligibly small. Roberts [5] and Gasanov [4] subsequently showed that for thin films, impurity levels introduce no significant modification to the rectangular shape predicted by Geppert's simplified analysis. The neglect of image forces, surface states, traps, and other effects is implicit in Fig. 1 in which the film is represented by a rectangular potential hill, height Φ and width s . We shall adopt this simple model to obtain the essential features of TAT. Clearly it is electron transfer which proceeds at levels below Φ which is relevant to our present discussion.

At a given energy ε , the tunnelling current may be expressed as

$$J(\varepsilon) = e n(\varepsilon) v(\varepsilon) P(\varepsilon),$$

where n and v represent the concentration of electrons and their velocity respectively and P is the barrier transmission coefficient. The charge arriving at the cathode per unit area per second, $e n(\varepsilon) v(\varepsilon)$, is described by the Fermi-Dirac distribution function, $f(\varepsilon)$, so that the current may alternatively be written as the product of two integrals [11]:

$$J(\varepsilon) = \frac{4 \pi m e}{h^3} \int_0^\infty f(\varepsilon) d\varepsilon \int_0^{E_t + \Phi} P(\varepsilon) d\varepsilon, \quad (3)$$

where m is the electron mass and h represents Planck's constant.

In order to confine the analysis to energy differences we define a new energy parameter,

$$E = \varepsilon - E_t,$$

where E_t is the Fermi level energy.

We then make use of the following approximate expression for the transition probability, derived from a W.K.B. approximation [30]:

$$\log P(\varepsilon) = - \int_0^s \left[\frac{8 m}{\hbar^2} \{ \Phi(x) - E \} \right]^{1/2} dx. \quad (4)$$

Our simplifying assumption of a trapezoidal shaped barrier due to the presence of an applied field, F , means that $\Phi(x)$, the barrier height in the region above the metal Fermi level may be equated to $\Phi - Fx$, with $F = eU/s$.

Integrating (4) then yields

$$\log P(\varepsilon) = - \left[\frac{2}{3} \sqrt{\frac{8 m}{\hbar^2}} \frac{1}{F} (\Phi - E - Fx)^{3/2} \right]_0^s. \quad (5)$$

For $\Phi > eU$, $J = J_{\text{FLT}} + J_{\text{TAT}}$. The former includes all contributions to the tunnelling current arising from charge traversing the full thickness of the dielectric, the limits of integration being $(-E_f)$ and $(\Phi - eU)$. The remainder of the current, $J - J_{\text{FLT}}$, originates from the upper part of the barrier where electrons of different energies traverse different thicknesses of the barrier. The energy bounds of this thermally assisted tunnelling current are, $(\Phi - eU)$ and Φ .

Substituting (5) into (3) and using the relation

$$f(\epsilon) = \frac{E + E_f}{1 + e^{E/kT}},$$

we obtain

$$J_{\text{FLT}} = \frac{4\pi m e}{h^3} \int_{-E_f}^{\Phi - eU} \left(\frac{E + E_f}{1 + e^{E/kT}} \right) \times \\ \times \exp \left\{ -\frac{2}{3} \sqrt{\frac{8m}{h^2}} \frac{1}{F} [(\Phi - E)^{3/2} - (\Phi - E - sF)^{3/2}] \right\} dE \quad (6a)$$

and

$$J_{\text{TAT}} = \frac{4\pi m e}{h^3} \int_{\Phi - eU}^{\Phi} \left(\frac{E + E_f}{1 + e^{E/kT}} \right) \exp \left\{ -\frac{2}{3} \sqrt{\frac{8m}{h^2}} \frac{1}{F} (\Phi - E)^{3/2} \right\} dE. \quad (6b)$$

To obtain current-voltage characteristics appropriate to tunnelling in the two distinct regions, now necessitates numerical integration of (6a) and (6b) for particular sets of parameters. We can, however, approximate these expressions and obtain analytical expressions for certain limiting cases of interest.

A guide as to the relative importance of FLT and TAT may be found by comparing the maximum terms in each integral. For direct tunnelling it is a good first approximation to assume that the largest component of the integral in (6a) comes from the energy level, $E = 0$. The maximum term may then be written

$$J_{\text{FLT}} (\text{max}) \approx \frac{4\pi m e}{h^3} E_f \exp \left\{ -\frac{2}{3} \sqrt{\frac{8m}{h^2}} \frac{1}{F} [\Phi^{3/2} - (\Phi - F s)^{3/2}] \right\}. \quad (7)$$

For a realistic set of parameters it is easy to show that the main contribution to TAT comes from energies that are well above the Fermi energy, $E \gg 0$. Fermi-Dirac statistics can then be approximated by Maxwell-Boltzmann statistics and the function within the integration sign can be differentiated to obtain the following criterion for the maximum term (we consider regions where the second derivative is negative):

$$E_{\text{max}} = \Phi - \left(\frac{F^2}{k^2 T^2} \right) \frac{h^2}{8m}. \quad (8)$$

Therefore,

$$J_{\text{TAT}} (\text{max}) \approx \frac{4\pi m e}{h^3} (E_{\text{max}} + E_f) \exp \left\{ -\frac{\Phi}{kT} + \frac{1}{3} \frac{F^2}{k^3 T^3} \frac{h^2}{8m} \right\}. \quad (9)$$

A comparison of the exponential factors in the integrands gives

$$\log \frac{J_{\text{TAT}}}{J_{\text{FLT}}} \approx \log \frac{J_{\text{TAT}}(\text{max})}{J_{\text{FLT}}(\text{max})} = \log J_{\text{R}} = \frac{2}{3} \sqrt{\frac{8m}{\hbar^2}} \frac{1}{F} [\Phi^{3/2} - (\Phi - Fs)^{3/2}] - \frac{1}{kT} \left[\Phi - \frac{1}{3} \frac{F^2}{k^2 T^2} \left(\frac{\hbar^2}{8m} \right) \right]. \quad (10)$$

In the following section we present some results for J_{R} and compare them with accurate values obtained by numerically integrating (6a) and (6b).

Another method of approximation is to simplify the integrand and also restrict the range of integration. For example, (6a) is valid for $E \ll \Phi - eU$. By taking the first term in the binomial expansion for $(\Phi - E)^{3/2}$ and integrating between say $-5kT$ and $+5kT$, one can obtain an approximate analytical solution for the complete FLT integral.

4. Numerical Results

Most of this section describes computer curves we have obtained for situations where thermally assisted tunnelling is the dominant conduction mechanism in the solid. However, in order to illustrate the distinction between FLT and TAT we present in Fig. 2 a plot of the individual components of each integral in

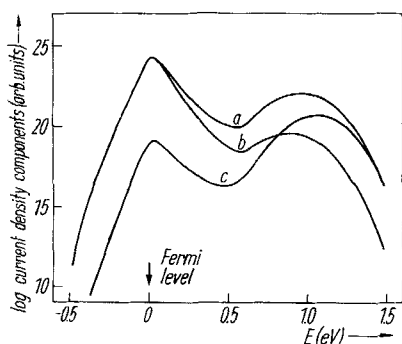


Fig. 2. Individual current components of the total current integral as a function of energy displacement from the Fermi level, for a model with $\Phi = 1.5$ eV, $U = 0.9$ V. (a) $s = 45$ Å, $T = 300$ °K, $J = 4.34 \times 10^{-12}$ A/cm²; (b) $s = 50$ Å, $T = 300$ °K, $J = 2.51 \times 10^{-11}$ A/cm²; (c) $s = 45$ Å, $T = 280$ °K, $J = 3.00 \times 10^{-13}$ A/cm².

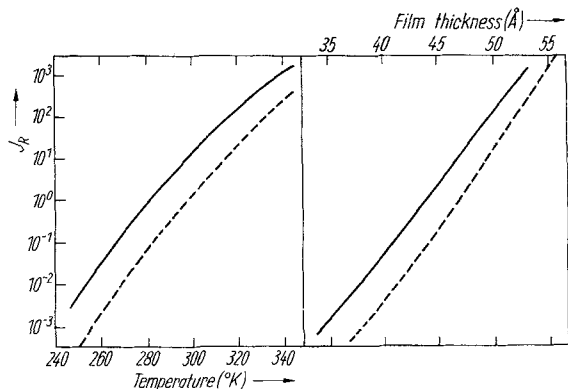


Fig. 3. Comparison of FLT and TAT in a model with $\Phi = 1.5$ eV, $U = 0.81$ V, for a range of temperatures and thicknesses

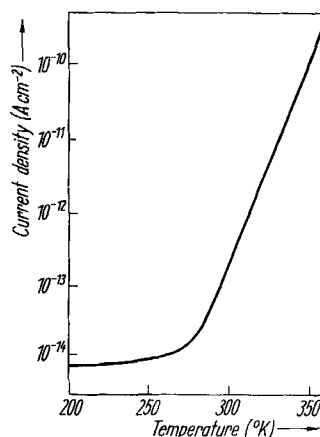


Fig. 4. Temperature variation of the current for constant voltage, 0.86 V, in a film with $\Phi = 1.5$ eV, $s = 50$ Å

equations (6) as a function of E . The integrations were carried out using a Simpson's rule procedure. Two distinct peaks are evident for each curve, one corresponding to direct tunnelling near the Fermi level energy and the other arising from thermally assisted tunnelling. Clearly, in view of the importance of both mechanisms in all three cases, a study of the voltage, temperature, and thickness dependence of the total current would provide complicated relationships. Curves a and b indicate, for example, how an increase in thickness of 5 Å is sufficient to replace FLT by TAT as the dominant conduction mechanism in the dielectric. In a similar way, an increase in temperature can enhance the TAT term and suppress the importance of the FLT effect. This is demonstrated in Fig. 3 where the ratio $J_R = J_{\text{TAT}}/J_{\text{FLT}}$, is plotted as a function of both temperature and thickness for a model with $\Phi = 1.5$ eV and 0.81 V applied. As may be expected, for low temperatures and/or very thin films, Fermi level tunnelling dominates, but for temperatures greater than 300 °K and thicknesses > 50 Å, thermally assisted tunnelling controls the characteristic. It is possible of course that in a practical situation, another mechanism might manifest itself under those conditions and thus obscure the TAT effect. Nevertheless, these curves indicate that in situations where it is suspected that direct tunnelling ceases to be of importance [13, 21], the alternative tunnelling mechanism proposed should be considered.

A guide as to when TAT starts playing a role may be found from (10) by calculating J_R . The dotted curves in Fig. 3, indicate that our approximate expression for this parameter can underestimate the effect of TAT by almost an order of magnitude. J_R , essentially arises from a direct comparison of the peak values of the two Gaussian type curves in Fig. 2. The discrepancy is therefore probably due to the broader shape of the TAT curve coupled with our disregard of the pre-exponential factors.

The transition from FLT to TAT is also clearly evident in Fig. 4. The relatively weak temperature dependence of the current up to approximately 270 °K is a consequence of the dominant FLT integral within this range of temperature. The sharp transition signifies that for higher temperatures, the FLT integral is always subordinate to the TAT integral. The characteristic is similar to that reported by Pollack [21] for a Pb-Al₂O₃-Pb film and interpreted by him in terms of a transition from tunnelling to thermionic emission. The lower values of current in our plot are a consequence of the larger barrier height chosen.

The rest of this section deals only with TAT. It will be implicit that any further illustrations describe models with appropriately chosen parameters to make TAT the dominant tunnelling mechanism in the dielectric.

In the main we treat thin barriers ≈ 100 Å thick but thicker barriers ≈ 5000 Å which also exhibit similar J - U characteristics provided $eU < \Phi$, are also used to illustrate the effect. In the latter case, the limits of integration proposed in the previous section do not apply as we are now in the domain of field emission. However, the maximum term in the integral is located very close to the top of the barrier and the current can thus be classified as being due to thermally assisted tunnelling.

Fig. 5a shows typical current-voltage curves at various temperatures computed from the integrals in (6) for a model with $\Phi = 0.8$ eV and thickness 75 Å. It is important to notice the linear relationship between $\log J$ and $U^{1/2}$, i.e. *for appropriate parameters, thermally assisted tunnelling yields the same shape current-voltage characteristic as Schottky emission or the Poole-Frenkel effect.*

It may be seen that the extent of the linear regions narrows as the temperature is decreased. The non-linear part of the characteristic may be described by a $\log J \sim U^{3/2}$ law. This is illustrated in Fig. 5b for the 200 °K curve. Fig. 6, which shows J - U curves for a range of thicknesses, illustrates the point we made previously regarding thicker films exhibiting the same kind of TAT behaviour as thin films, although it is in these situations where $\Phi = 1$ eV, $T = 300$ °K and thicknesses are typically ≈ 5000 Å where, in practice one would expect bulk effects to manifest themselves. Two features of these curves are the change of slope, B , both with temperature and thickness of film, and also the intercept on the $U = 0$ axis of the curves in Fig. 6. It is instructive

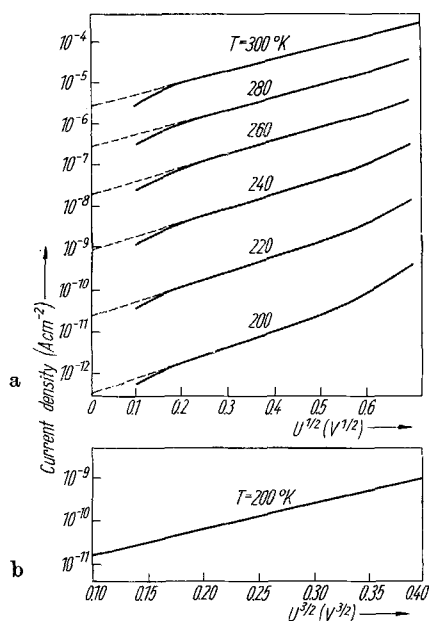


Fig. 5. Conductivity curves at various temperatures computed from equation (6) for a model with $\Phi = 0.8$ eV and $s = 75$ Å

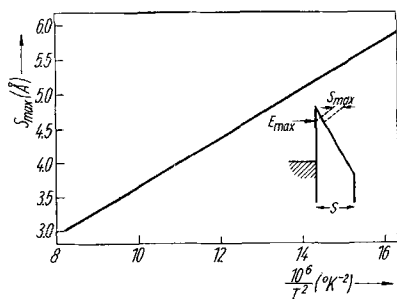


Fig. 8. Temperature variation of s_{\max} , for a film with $\Phi = 1$ eV, $U = 17$ V and $s = 6000$ Å

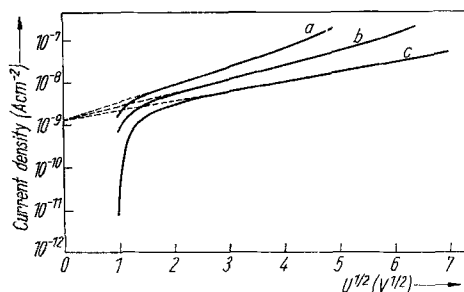


Fig. 6. Conductivity curves for various thicknesses; $\Phi = 1$ eV, $T = 300$ °K. (a) $s = 3000$ Å; (b) $s = 5000$ Å (c) $s = 10000$ Å

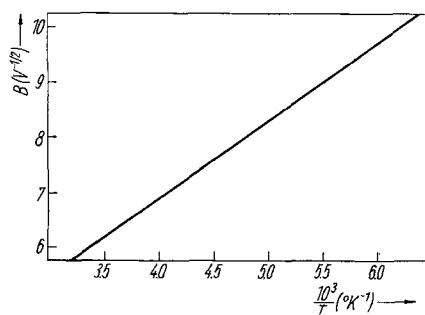


Fig. 7. The variation with temperature of the slope B , of the conductivity curves in Fig. 5

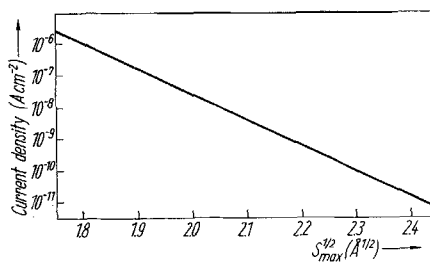


Fig. 9. Variation of $s_{\max}^{1/2}$ with current for the model described in Fig. 8

to investigate these variations and compare them with the relations which hold for the Schottky effect.

Firstly in Fig. 7 we show the variation of slope of the current-voltage curves in Fig. 5 as a function of $1/T$. Direct tunnelling is of course weakly dependent on temperature but a variation similar to that shown in this diagram is to be expected for TAT. We can explain the linear relationship in the following way: If we assume that the main contribution to the TAT integral in equation (6a) originates at the energy level E_{\max} , (see equation (8) and Fig. 8) then electron transfer will occur predominantly across a corresponding region, s_{\max} wide. Tunnelling is strongly dependent on thickness and therefore, as E_{\max} moves with temperature with a resulting change in s_{\max} , the tunnelling current will clearly be a function of temperature.

By simple proportion using (8) one obtains

$$s_{\max} = \frac{1}{8} \frac{e U}{s} \frac{\hbar^2}{k^2 T^2 m}. \quad (11)$$

One may regard s_{\max} as the 'effective thickness' of the film which depends on both temperature and applied voltage. Although it is important to stress the fact that we are dealing with a distinct mechanism to Schottky emission, the concept of an effective thickness and the resulting effective barrier

$\left(\Phi - \frac{1}{3} \frac{F^2}{k^2 T^2} \left(\frac{\hbar^2}{8 m} \right) \right)$ suggested by (9), is very reminiscent of the conventional expression for thermionic emission in insulators.

The linear dependence of s_{\max} on $1/T^2$ is illustrated in Fig. 8 and the square root dependence of s_{\max} on $\log J$ in Fig. 9. A combination of these relations yields the required dependence on temperature shown in Fig. 5. s_{\max} , involves the field $F = e U/s$, and as such, to be consistent with the findings of Fig. 5 and 9 and equation (11), one must expect to find a linear relationship between $\log J$ and s^{-1} . This is borne out from our numerical results.

5. Discussion

A temperature dependent current flow which increases exponentially with the square root of the applied voltage for large electric fields is usually ascribed to either Schottky or field assisted thermal emission. Tunnelling is usually dismissed as a contributory factor owing to the temperature dependence and in some cases the thickness of the film. We have indicated in the previous sections that thermally assisted tunnelling may yield the exact same current-voltage characteristics. It is unfortunate that the appropriate equations cannot have been solved analytically to enable a complete determination to be made of the functional relationship between the various parameters. However, the numerical results suggest that an empirical relation of the form

$$J_{\text{TAT}} = a \exp \left\{ -\frac{\Phi}{kT} \right\} \exp \left\{ \left(\frac{b}{kT} + c \right) \frac{U^{1/2}}{s^{1/2}} \right\}, \quad (12)$$

where $a = 6.8 \times 10^7 \text{ A/cm}^2$, $b = 1.65 \times 10^{-24} \text{ J m}^{1/2}/\text{V}^{1/2}$ and $c = 1.2 \times 10^{-4} \text{ m}^{1/2}/\text{V}^{1/2}$, describes thermally assisted tunnelling. These values, which represent the best fit to our computer curves, varied by only $\pm 3\%$ for the data obtained. In view of the relation illustrated in Fig. 5b it is likely that, at higher fields, an

additional term in $U^{3/2}$ would have to be introduced to describe TAT. One would, of course, expect the constants given above to be critically dependent on the shape of the barrier.

Direct comparison of (2) and (12) show an equivalence with the Schottky effect when $a = A T^2$ and $(c + b/kT) = (e^3/\kappa)^{1/2}/kT$. These relations yield a temperature ≈ 750 °K and a dielectric constant ≈ 8 at room temperature. It is also instructive to compare the values of J_{TAT} and the Schottky current, J_{SCH} , (at different temperatures) for $\kappa = 1$ and a field which yields a linear $\log J$ versus $U^{1/2}$ plot, e.g. 2×10^5 V/cm.

$$T = 400 \text{ °K}, \quad J_{\text{TAT}}/J_{\text{SCH}} = 2.6;$$

$$T = 300 \text{ °K}, \quad J_{\text{TAT}}/J_{\text{SCH}} = 4.1;$$

$$T = 200 \text{ °K}, \quad J_{\text{TAT}}/J_{\text{SCH}} = 7.3.$$

For all these cases, TAT controls the current-voltage characteristic. However, for higher values of field, the Schottky effect increases more rapidly with applied field than TAT so that thermionic emission eventually becomes dominant.

It is possible to distinguish between TAT and conventional thermionic emission by extrapolating the linear regions of $\log J$ versus $U^{1/2}$ curves to zero voltage (in some cases [13], the focal point of the linear regions for various thicknesses lies at a positive voltage; in these instances an appropriate correction would have to be made) and calculating the barrier height, Φ , according to either (2) or (12). The correct form of equation would yield a constant value of Φ . An interesting deduction is that, should TAT be incorrectly interpreted in terms of the Schottky effect, then for realistic temperatures, the result obtained for Φ would always underestimate the height of the barrier. It is interesting to note that barrier heights deduced experimentally from assumed Schottky plots are invariably lower than the values obtained from other measurements e.g. the threshold for photo response. The distinction between TAT and the Poole-Frenkel effect should also prove to be possible experimentally although the added complication of a field-dependent pre-exponential term could complicate matters in this case. Brown et al. [31] have interpreted their experimental results in terms of the latter although two features of their curves are more characteristic of TAT than the Poole-Frenkel effect. Firstly, the pre-exponential factor is independent of voltage and secondly, deviations from linear $\log J$ versus $U^{1/2}$ behaviour are observed at low temperatures and high fields.

Table 1 compares the values of Φ obtained from the zero-voltage intercept and equation (12) — Φ_0 and the Schottky effect — Φ_{SCH} for the experimental curves reported by Hartman et al. [29]. While $\Phi_0 > \Phi_{\text{SCH}}$ for all temperatures, it is not a constant and consequently these curves do not conform to either the Schottky or TAT relations. This could be indicative of the co-existence of these two mechanisms in these experiments.

It is evident that for TAT, using equation (12), a general table (Table 2) can be drawn up relating the current density at the $U = 0$ intercept to barrier height. Another consequence of (12) is the hypothetical dielectric constant value, eight, which is weakly dependent on temperature.

The two terms in the exponent of (12) could be considered as describing the concentration of electrons available for tunnelling (proportional $\exp - \Phi/kT$) and a tunnelling factor $\exp (b/kT + c) U^{1/2}/s^{1/2}$. Temperature is involved in

Table 1

Comparison of the barrier height deduced from the zero voltage intercept in Fig. 3 (Hartmann et al. [29] using equation (2) — Φ_{SCH} and equation (12) — Φ_0)

T ($^{\circ}\text{K}$)	J (A^2/cm^2)	Φ_0 (eV)	Φ_{SCH} (eV)
297	2.7×10^{-8}	0.9	0.86
270	5.6×10^{-9}	0.86	0.81
221	8.0×10^{-11}	0.79	0.74
195	6.2×10^{-12}	0.74	0.69

Table 2

TAT current density in A/cm^2 at the zero voltage intercept predicted by equation (12) for rectangular barrier model

T ($^{\circ}\text{K}$)	Φ (eV)			
	0.7	0.8	0.9	1.0
200	1.55×10^{-10}	4.69×10^{-13}	1.42×10^{-15}	4.25×10^{-18}
260	1.83×10^{-6}	2.11×10^{-8}	2.43×10^{-10}	2.80×10^{-12}
300	1.18×10^{-4}	2.46×10^{-6}	5.15×10^{-8}	1.07×10^{-9}

the latter term only because s_{max} , is temperature dependent in the rectangular barrier model. However, one could envisage a situation in which, owing to space charge effects, the barrier contained a region in which the effective thickness near the top of the barrier was not a linear function of energy in the barrier but approximated more closely to a constant. In this case, although E_{max} might change with temperature, s_{max} , and thus the tunnelling part of equation (12) could depend only weakly on temperature. (The modified barrier shape would presumably result in the constant, c , in (12) dominating the exponential factor). This could explain the experimental results [25, 26] quoted earlier in the paper, in which the slope of the $\log J$ versus $U^{1/2}$ plots remained temperature independent over a large range of temperature. The Schottky effect, even including modifications to the barrier shape, could never explain such behaviour.

6. Conclusions

The theoretical curves we have presented for thermally assisted tunnelling indicate that, for appropriate parameters, TAT yields the same shape current-voltage characteristic as Schottky emission or the Poole-Frenkel effect. Careful measurements could distinguish between these mechanisms but differences might well be obscured experimentally by changes in the solid such as barrier shape with applied voltage. The results summarized in equation (12), suggest that an interpretation of a characteristic due to TAT, in terms of Schottky emission, would yield a dielectric constant of approximately eight and an underestimate of the barrier height. The former would depend strongly on the shape adopted for the barrier. Our major conclusion should, however, be valid irrespective of the particular model chosen and therefore TAT must be considered in.

investigations of thin film dielectrics. The theory might also be relevant to the problems of charge transfer across intermolecular barriers in organic solids and switching and memory effects in solids. We have, in fact, observed switching behaviour to a higher conductivity state in single crystal naphthalene. Work on these topics in this department is projected or in hand.

Acknowledgements

The authors are indebted to Dr. G. Lucovsky for his suggestions in formulating the TAT problem. We also acknowledge his assistance in kindly permitting us access to some of his unpublished experimental results and for helpful discussions.

References

- [1] D. V. GEPPERT, *J. appl. Phys.* **34**, 490 (1963).
- [2] D. V. GEPPERT, *J. appl. Phys.* **33**, 2993 (1962).
- [3] J. ANTULA, *phys. stat. sol.* **28**, 395 (1968).
- [4] L. S. GASANOV, *Fiz. Tekh. Poluprov.* **1**, 809 (1967).
- [5] G. G. ROBERTS, *Brit. J. appl. Phys.* **18**, 749 (1967).
- [6] F. W. SCHMIDLIN, *J. appl. Phys.* **37**, 2823 (1966).
- [7] J. G. SIMMONS, *Brit. J. appl. Phys.* **18**, 269 (1967).
- [8] J. G. SIMMONS, *Phys. Rev.* **155**, 657 (1967).
- [9] J. R. YEARGAN and H. L. TAYLOR, *J. appl. Phys.* **39**, 5600 (1968).
- [10] J. ANTULA, *phys. stat. sol.* **24**, 89 (1967).
- [11] D. R. LAMB, *Electrical Conduction Mechanisms in Thin Insulating Films*, Methuen and Co. Ltd., London 1967.
- [12] J. J. O'DWYER, *J. appl. Phys.* **37**, 599 (1966).
- [13] N. MCCOLL and C. A. MEAD, *Trans. MS AIME*, **233**, 502 (1965).
- [14] P. R. EMTAGE, *J. appl. Phys.* **38**, 1820 (1967).
- [15] R. A. KELLER and H. E. RAST, *J. chem. Phys.* **36**, 2640 (1962).
- [16] R. H. TREDGOLD, *Proc. Phys. Soc.* **80**, 807 (1962).
- [17] J. C. FISHER and I. GIAEVER, *J. appl. Phys.* **32**, 172 (1961).
- [18] A. SOMMERFELD and H. BETHE, *Hdb. Phys.*, Springer-Verlag, Vol. XXIV, Berlin 1933 (p. 450).
- [19] R. STRATTON, *J. Phys. Chem. Solids* **23**, 1177 (1962).
- [20] P. R. EMTAGE and W. TANTRAPORN, *Phys. Rev. Letters* **8**, 267 (1962).
- [21] S. R. POLLACK, *J. appl. Phys.* **34**, 877 (1962).
- [22] T. W. HICKMOTT, *J. appl. Phys.* **37**, 4380 (1966).
- [23] A. SUSSMAN, *J. appl. Phys.* **38**, 2738 (1967).
- [24] J. L. HARTKE, *J. appl. Phys.* **39**, 4871 (1968).
- [25] R. W. CHRISTY, *J. appl. Phys.* **35**, 2179 (1964).
- [26] G. LUCOVSKY, unpublished results on Ta-Ta₂O₅-Al structures.
- [27] A. C. LILLY, JR., D. A. LOWITZ, and J. C. SCHUG, *J. appl. Phys.* **39**, 4360 (1968).
- [28] H. HIROSE and Y. WADA, *Japan J. appl. Phys.* **4**, 639 (1965).
- [29] T. E. HARTMAN, J. C. BLAIR, and R. BAUER, *J. appl. Phys.* **37**, 2468 (1966).
- [30] N. F. MOTT and I. N. SNEDDON, *Wave Mechanics and Its Applications*, Dover/New York 1963 (p. 23).
- [31] G. A. BROWN, W. C. ROBINETTE, JR., and H. G. CARLSON, *J. Electrochem. Soc.* **115**, 948 (1968).

(Received November 21, 1969)